

Be erosion and migration with isotopic effect observed in JET-ILW

D.V.Borodin¹, T.Dittmar¹, R.Henriques², E.Pawelec³, E. de la Cal⁴, S. Silburn⁵,
J.Romazanov¹, A.Shaw⁵, A.Meigs⁵, K.Lawson⁵, S.Brezinsek¹, I.Borodkina⁶, D.Douai⁷,
A.Huber¹ and JET contributors*

¹Forschungszentrum Jülich GmbH, Institut für Energie- und Klimaforschung – Plasmaphysik, Partner of the Trilateral Euregio Cluster (TEC), 52425 Jülich, Germany; ²Instituto de Plasmas e Fusão Nuclear, Instituto Superior Técnico, Universidade de Lisboa, Lisboa, Portugal; ³University of Opole, Institute of Physics, Oleska 48, Opole, Poland; ⁴CIEMAT, Avda. Complutense, 40, Madrid 28040, Spain; ⁵UK Atomic Energy Authority, Culham Science Centre, Abingdon, OX14 3DB Oxfordshire, UK; ⁶Institute of Plasma Physics of the CAS, Za Slovankou 3, 182 00 Prague 8, Czech Republic; ⁷CEA, IRFM, F-13108, Saint-Paul-Lez-Durance, France

*See the author list of E. Joffrin et al. 2019 Nucl. Fusion 59 112021

1. Introduction.

The JET ITER-like wall (ILW) with beryllium (Be) main chamber provides the most relevant for ITER tokamak environment for studying Be erosion [1] and its migration into the tungsten (W) divertor, which largely determines W erosion critical for the plasma operation [2]. Moreover, co-deposition of tritium (T) with Be is the largest contribution to T retention in the wall [3], which must be kept below the safety limit. The present contribution is largely focused on the differences in Be erosion yields in H/D/T plasmas based on experiments and modelling.

An extrapolation from JET to ITER [4, 5, 6] of the processes mentioned and their interplay demands numeric modelling. Relevant tools like ERO2.0 [7] code (erosion/migration, gyro-resolved transport of impurities in the context of the 3D-shaped wall) as well as e.g. Edge2D-EIRENE (providing relevant plasma backgrounds) [8] are highly developed, however require validation experiments for each case at hand to reduce uncertainties characteristic for fully *ab initio* calculations. Moreover, certain processes like chemically assisted physical sputtering (CAPS) of Be demand further experimental investigation as well as effects on physical sputtering (PS) of plasma isotopes, wall temperature and content, etc.

The earlier experiment in D plasma has shown [9] that increasing of surface temperature T_{surf} can lead to full suppression of CAPS with a clear indication that this effect is related to the increased outgassing from the surface. Later on [10, 5] this was reproduced by the modelling.

Aim of this work was to confirm the erosion yields for Be, study the contributions of CAPS and PS to the total Be sputtering yield and to get the validation experiments for Be migration inside the JET vessel including the role of the Be-containing molecules released.

2. Experiment: Be CAPS in H and D plasma.

T_{surf} is one of the key parameters for determining the fraction of CAPS in the total Be erosion. Similar to the earlier experiment [9] it was scanned by heating the wall with consecutive pulses. The repetition rate was such that cooling between the pulses was mostly smaller than the heating during the inner wall (IW) limited pulses (types 2, 4 listed below) with long-inward shifted plasma phases. Here, the T_{surf} scan was done at somewhat higher T_e , thus ion impact energy E_{in} than in [9]. Moreover, for Be migration studies few additional pulse types were used with repetitions to get a second set of interference-filtered 2D camera images:

- 1) Be monitoring pulses, “BeMP” [11] (limiter, diverted ohmic, L-mode, H-mode) containing ~2s flat tops. Neutral beam heating was not available in H campaign, so density steps in ohmic plasma were done instead of L- and H-mode phases.
- 2) Heating pulses (long constant plasma limiter pulses), suitable for measurements.
- 3) Density scans: varied fuelling in the fixed limiter magnetic configuration (determining for T_e) to study the $Y(E_{in})$ yield dependence.

4) Combi-pulses: heating + elements of 1) or 3) for measurements.

Type 1, 3 pulses were done at the beginning of the session (cold wall, maximal CAPS) and, if possible, closer to the end of the session with at least partially suppressed CAPS. Heating of the IW Be limiters during the BeMPs was negligible.

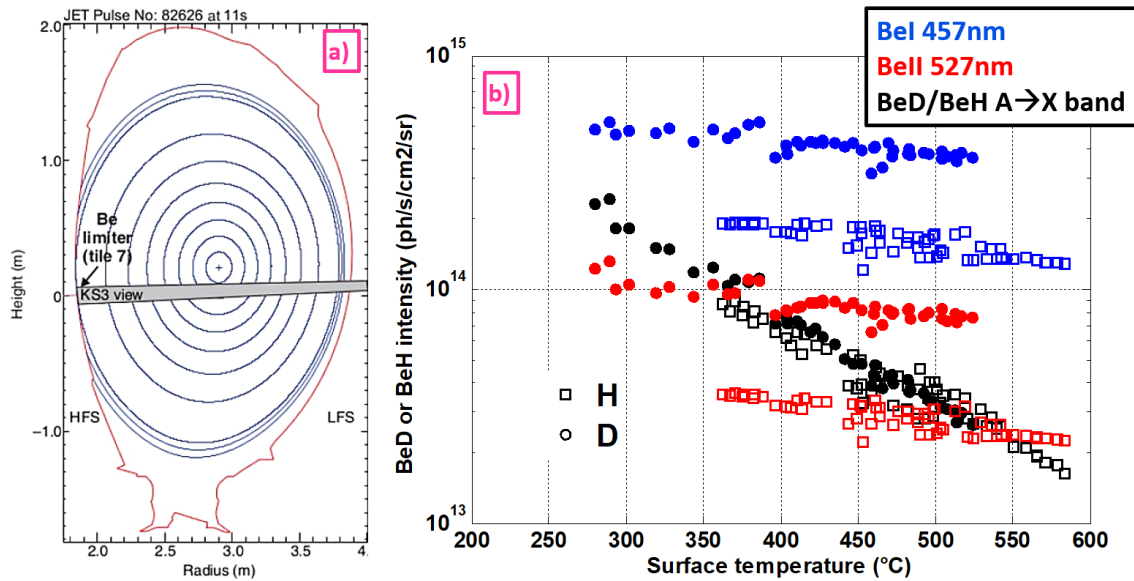


Fig.1. a) Projection of the “KS3 view” sightline to the poloidal plane of JET. b) The integrated line intensities in this sightline for selected BeI, BeII lines and BeD band characterising the influx of those species from the inner wall guard limiter made of solid Be. Empty squares are for sessions in H plasmas, dots are for D plasmas.

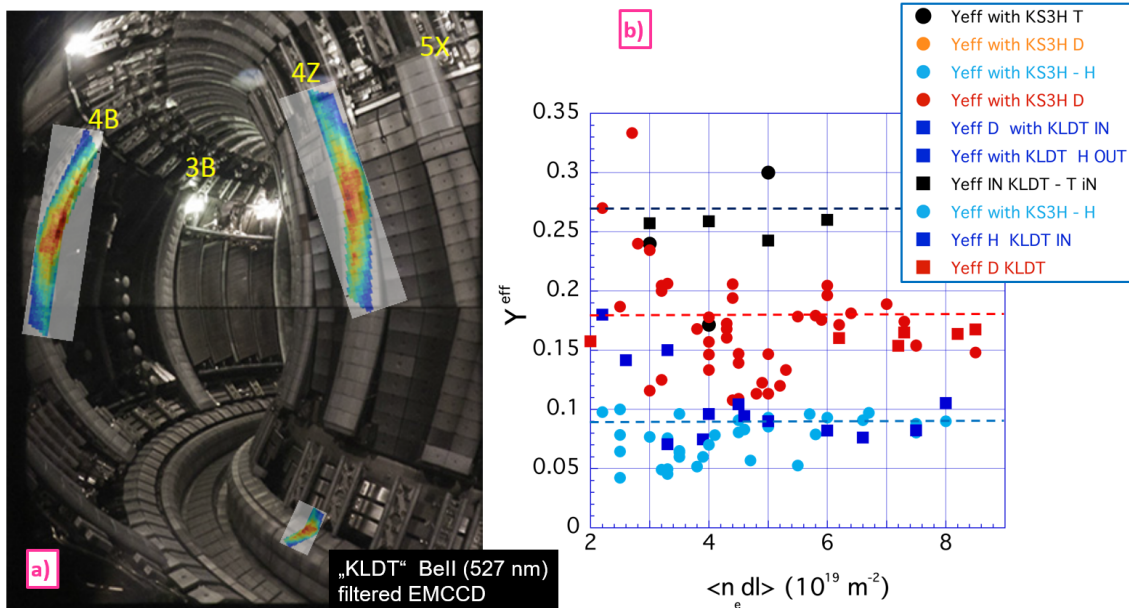


Fig.2. a) The 2D camera view into the JET vessel with ROIs indicated by representative examples of BeII light emission patterns (few other filters were used on this and other similar cameras). b) the sputtering yields obtained by the S/XB method based on integrated intensities in H, D and T plasmas inside inner wall (“in”) and outer wall (“out”) ROIs plotted against line-averaged electron density n_e .

The infrared (IR) camera measurements T_{surf} were cross-calibrated with the thermocouple measurements inside the bulk for both H and D experiments. Also the appropriate regions of interest (ROIs) on the IW limiters inside the 2D IR images were selected.

The first phase of the analysis completed is presented in **Fig.1**. The spectral intensities integrated in just one of multiple JET sightlines (**Fig.1a**) are shown. However probably the

most representative one as it “looks” just at the point of maximal erosion close to the contact point at the IW (see Fig. 3). The measurement and interpretation of the BeD A-X band fraction including H/D/T isotope effects is described in detail in [12]. This intensity is characteristic for the BeD release due to the CAPS, which occurs to be very similar even by the absolute magnitude in both H and D pulses. It should be noted that despite the pulses in D and H were performed in precisely the same magnetic configuration, the respective CAPS yields need to be accounted for plasma parameters which interpretive modelling is still ongoing. This can reveal potential differences in the sputtering specie fluxes (H or D) at relevant locations. On the other hand, these fluxes are proportional to the plasma density, the same way as the light emitted by the released impurities, thus respective corrections might compensate each other. At any rate, the CAPS yields $Y_{BeD \leftarrow D/H}$ in D and H plasmas are proportional to each other $Y_{BeD \leftarrow D} \sim Y_{BeD \leftarrow H}$, close in magnitude and reveal suppression at the same IW T_{surf} above 550°C . The atomic lines, BeI 457nm characterising the local influx of the neutral Be as well as BeII 527nm characterising the ionised Be which comes into the sightline also from the other IW guard limiters are much less dependent on T_{surf} as only a fraction of these impurities is due to the BeH and BeD decay, respectively. The values at high T_{surf} with suppressed CAPS characterize the pure PS of Be including the self-sputtering, which is proportional to the concentration of Be in plasma f_{Be} . Neglecting the difference in light emissivities due to different T_e in H and D plasmas the ratio $Y_{Be \leftarrow D} + f_{Be}(D) * Y_{Be \leftarrow Be} / Y_{Be \leftarrow H} + f_{Be}(H) * Y_{Be \leftarrow Be}$ appears to be $\sim 2.7-2.8$, which is considerably larger than SDTrimSP [13] calculated $Y_{Be \leftarrow D} / Y_{Be \leftarrow H}$ which is below 2 in the relevant E_{in} range. The latter indicates significantly larger f_{Be} in D plasma.

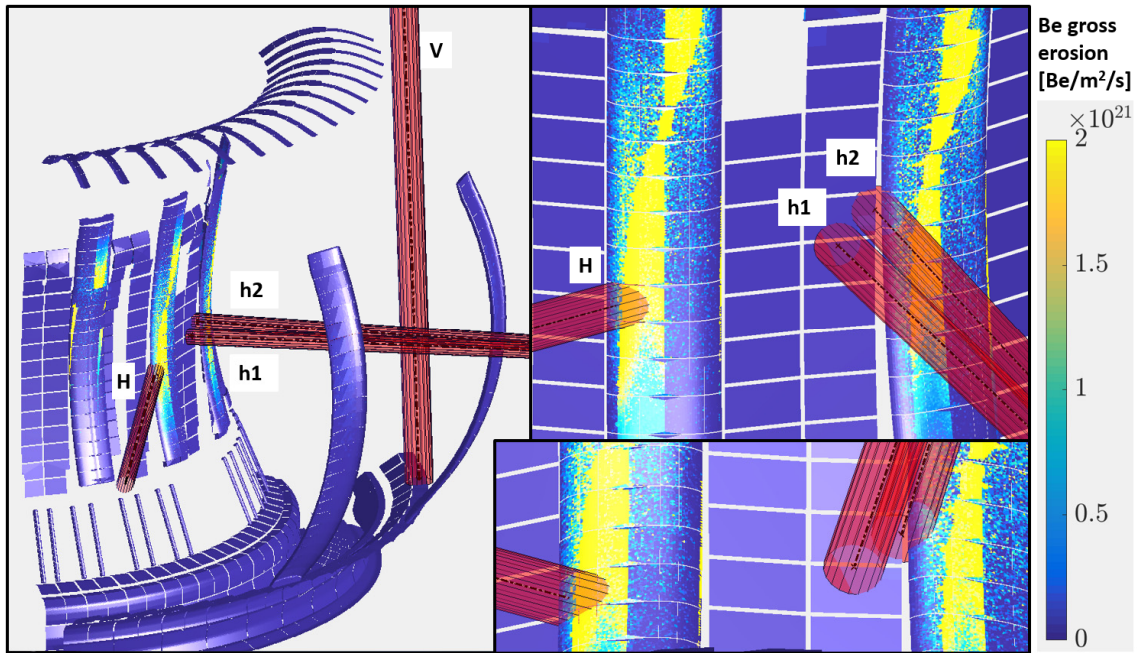


Fig.3. ERO2.0 is 3D Monte-Carlo impurity transport and plasma-surface interaction code simulations [11] for Be erosion along the JET ILW. 4 JET passive spectroscopy sightlines (“H” is also known as “KS3 bunker view” shown in Fig.1a.) are incorporated. The simulations show different trends for the intensities of any of the selected lines during a plasma parameter scan, thus those signals provide vast validation material. In addition, ERO2.0 is capable to simulate images from 2D cameras with spectroscopic filters and even IR images determined by the head loads along the FW with impact of magnetic shadowing.

3. H/D/T isotope effect on Be erosion with the S/XB approach.

Assuming the local thermodynamic equilibrium (LTE) in a constant plasma one can estimate $S/XB(n_e, T_e)$ conversion factors [14] for the impurity influx from the wall

characterized by its line emission. *S/XBs* are available for instance in ADAS [15]. To get the effective yield one can assume that recycling of D/H flux is 100% and thus

$$Y_{Be \leftarrow D/H}^{Eff} = (S/XB_{BeII} * I_{BeII}) / (S/XB_{D\alpha} * I_{D-\alpha}) = R_c * I_{BeII} / I_{D-\alpha}, \quad (1)$$

where the coefficient R_c , specific for the selected combination of BeII 527nm and Balmer- α D/H line intensities (experimental signals). The S/XB method is known to be quite robust even if R_c dependence on (n_e, T_e) is neglected. **Fig.2b** presents the erosion yields estimated from eq. (1) assuming $R_c=1.8$ for the BeII 527nm line for a broader than in section 2 set of limiter pulses including some in T plasma. The data from the **Fig.1a** sightline is complemented with the data from the wide view camera with a filter for the same BeII line filter. The camera intensities were integrated along the selected ROIs at inner and outer wall as indicated in **Fig.2a**.

Fig.2b. clearly shows the significant isotope effect for the Be erosion in H/D/T plasmas. Moreover, the increase of the erosion in T is larger than could be expected just from the SDTrimSP calculated [13] PS yields just crudely proportional to the 1:2:3 isotope masses (less difference). As in the previous section, this is most probably self-amplifying effect of increased erosion due to contribution of the self-sputtering by the Be plasma impurity. However, due to the scarce number of analysed T plasmas more statistics is necessary to verify the yields.

Also the large scattering of the data is worth mentioning. The downside of the straightforward and robust S/XB approach is multiple explicit (mentioned above) and implicit assumptions. For instance, the local transport of the species, the optical properties of the observation system, plasma parameter and impurity concentration distributions inside the vessel may lead to geometry-dependent factors ζ_i between the $Y^{Eff} = Y * \zeta_i$ for any particular sightline or ROI and the universal yields Y which can be calculated [13] or extrapolated for ITER. The Be wall temperature at relevant locations, thus CAPS/PS ratio, is an additional uncertainty which was neglected. The detailed and precise interpretation of the data demands 3D modelling taking into account e.g. magnetic shadowing of 3D shaped wall like the one presented in **Fig.3**.

4. Summary and conclusion.

The CAPS contribution to the total Be erosion was investigated following the 2014 experiment in D plasma [9]. Be CAPS magnitude does not depend on H/D isotope. Full suppression at limiter both in D and H plasmas occurs at $T_{surf} \sim 550^\circ C$. This supports the hypothesis that D or H outgassing is the determining factor. Larger fraction of BeH to atomic release in H plasma than BeD in the D plasma is observed.

The isotopic effect for total Be erosion (largest for T, smallest for H) is shown by the S/XB approach applied to the combined data set from the selected sightline and ROIs from the 2D cameras with filters. The uncertainties in plasma parameters, geometry-dependent factors ζ_i for effective erosion yields and strong role of Be self-sputtering lead to large scattering of the data – numerical simulations are required for precise determination of the PS and CAPS yields.

The experiments have allowed to obtain systematic validation material for Be migration at various T_{surf} (and other parameters) in D and H plasmas.

Outlook. Next logical step in this work is a systematic comparison with the ERO2.0 simulations including for Be migration. Continuation of experiment in T plus additional session in D is expected (to obtain mostly full set of H/D/T data [16]).

- | | |
|--|---|
| [1] G. De Temmerman et al., Nucl. Mater. and Energy 27 (2021) 1009943 | [10] E Safi et al., J. Phys. D: Appl. Phys. 50 (2017) |
| [2] S. Brezinsek et al 2015 Nucl. Fusion 55 063021 | [11] J.Romazanov et al., NME 18 (2019) 331–338 |
| [3] A. Widdowson et al 2017 Nucl. Fusion 57 086045 | [12] E.Pawelec et al., this conference, P2.1024 |
| [4] D Borodin et al., 2011 Phys. Scr. 2011 014008 | [13] W.Eckstein, Top. Appl. Phys. 110 (2007), 33–187 |
| [5] D. Borodin et al., NME 19 (2019) 510–515 | [14] A Pospieszczyk et al 2010 J. Phys. B: At. Mol. Opt. Phys. 43 144017 |
| [6] J.Romazanov et al., NME 26 (2021) 100904 | [15] Summers, H. P. (2004) The ADAS User Manual, version 2.6 http://www.adas.ac.uk |
| [7] J.Romazanov et al., 2017 Phys. Scr. 2017 014018 | [16] D.Douai et al., invited at PFMC-20 |
| [8] H.A.Kumpulainen et al., NME 25 (2020) 100866 | |
| [9] S. Brezinsek et al 2014 Nucl. Fusion 54 103001 | |